

New states above charm thresholdEstia J. Eichten,^{1,*} Kenneth Lane,^{2,†} and Chris Quigg^{1,‡}¹*Theoretical Physics Department, Fermi National Accelerator Laboratory, P.O. Box 500, Batavia, Illinois 60510, USA*²*Department of Physics, Boston University, 590 Commonwealth Avenue, Boston, Massachusetts 02215, USA*

(Received 17 November 2005; published 19 January 2006)

We revise and extend expectations for the properties of charmonium states that lie above charm threshold, in light of new experimental information. We refine the Cornell coupled-channel model for the coupling of $c\bar{c}$ levels to two-meson states, defining resonance masses and widths by pole positions in the complex energy plane, and suggest new targets for experiment.

DOI: [10.1103/PhysRevD.73.014014](https://doi.org/10.1103/PhysRevD.73.014014)

PACS numbers: 14.40.Gx, 13.25.Gv, 14.40.Lb

I. INTRODUCTION

In the short time since the Belle Collaboration reported sighting the “missing” charmonium state $\eta_c'(2^1S_0)$ in exclusive $B \rightarrow KK_S K^- \pi^+$ decays [1], new states associated with charmonium have appeared in great profusion. Apart from the long-sought $h_c(1^1P_1)$, recently observed by the CLEO Collaboration in the decay $\psi(2S) \rightarrow \pi^0 h_c \rightarrow (\gamma\gamma)(\gamma\eta_c)$ [2,3], all the newly observed states lie near or above charm threshold. The identification of levels above the $D\bar{D}$ flavor threshold has renewed the importance of theoretical studies that couple the $c\bar{c}$ spectrum to charmed-meson–anticharmed-meson channels.

Motivated by the Belle Collaboration’s discovery [4] of the narrow state $X(3872) \rightarrow \pi^+ \pi^- J/\psi$, confirmed in short order by the CDF [5], D0 [6], and BABAR [7] experiments, we explored the influence of open-charm channels on charmonium properties and profiled the 1^3D_2 , 1^3D_3 , and 2^1P_1 charmonium candidates for $X(3872)$ [8]. We reaffirmed the single-channel potential-model expectation [9,10] that the favored 1^3D_2 and 1^3D_3 candidates both should have prominent radiative decays, and we noted that the 1^3D_2 might be visible in the $D^0 \bar{D}^{*0}$ channel, while the dominant decay of the 1^3D_3 state should be into $D\bar{D}$. We proposed that additional discrete charmonium levels were ripe for discovery as narrow resonances of charmed and anticharmed mesons. Barnes, Godfrey, and Swanson have reached similar conclusions using a different model for the coupling to open charm [11].

Experiments have enriched our knowledge of $X(3872)$, but its precise nature remains open to debate. On current evidence, $X(3872)$ is likely to be a $J^{PC} = 1^{++}$ state. If so, the surviving 2^3P_1 charmonium candidate is problematic, as we discuss in Sec. IV B 2. Not every state associated with charmonium need be identified as a $c\bar{c}$ state; we will mention below what some of the interlopers might be. An important goal of predicting the properties of charmonium states above flavor threshold is to tag new states that do not fit the template, and so might represent new spectroscopies.

Four other new particles require confirmation, for each has been seen only in a single experiment so far. Belle [12] has reported $Y(3943 \pm 11 \pm 13)$ in the decay $B \rightarrow K\omega J/\psi$; it is a relatively broad state, with total width $\Gamma = 87 \pm 22 \pm 26$ MeV. Belle also reports the state $X(3943 \pm 9)$, seen in $e^+e^- \rightarrow J/\psi + X$ [13]. It is observed to decay into $D\bar{D}^*$, but not $D\bar{D}$, which suggests an unnatural parity assignment. The total width is $\Gamma < 52$ MeV.

Belle has observed a narrow ($\Gamma \approx 20$ MeV) state in $\gamma\gamma \rightarrow D\bar{D}$ that they call $Z(3929 \pm 5 \pm 2)$ [14]. The production and decay characteristics are consistent with a 2^{++} assignment, and this state is a plausible $\chi'_{c2}(2^3P_2)$ candidate. The most recent addition to the collection is $Y(4260)$, a broad (≈ 88 MeV) 1^{--} level seen by BABAR in $e^+e^- \rightarrow \gamma\pi^+\pi^- J/\psi$ [15], with supporting evidence from $B \rightarrow K^- J/\psi\pi\pi$ [16].

In this paper, we fix the masses of the 3^1S_0 and 2^3P_2 charmonium states at the positions of $Y(3943)$ and $Z(3930)$, in order to sharpen our expectations for the properties of other states above charm threshold. We also extend our previous calculations to include additional states at higher masses. We highlight the search for narrow structures in charmed-meson–anticharmed-meson pairs, and we remark on analogue states to be expected in the $b\bar{b}$ spectrum.

II. EXPERIMENTAL STATUS

Let us briefly summarize what experiment has taught us about the new levels associated with charmonium, and how the experimental facts square with theoretical expectations.

A. Properties of η'_c

The hyperfine partner of $\psi(2S)$ now seems convincingly established, thanks to observations by the Belle [1,17], CLEO [18], and BABAR [19] experiments. The world-average values of the mass and width are $M(\eta'_c) = 3638 \pm 5$ MeV and $\Gamma(\eta'_c) = 14 \pm 7$ MeV [20].

The proximity of ψ' and η'_c to charm threshold means that communication with open-charm channels will alter the properties of these two narrow levels. As we elaborated in Ref. [8], the basic coupled-channel interaction is spin-

*Electronic address: eichten@fnal.gov†Electronic address: lane@bu.edu‡Electronic address: quigg@fnal.gov

independent, but the unequal masses and quantum numbers of the 2^3S_1 and 2^1S_0 potential-model eigenstates mean that their interaction with different charmed-meson—anticharmed-meson channels induces spin-dependent forces that affect the charmonium states. These spin-dependent forces give rise to S-D mixing that contributes to the $\psi(3770)$ electronic width, for example, and are a source of additional spin splitting.

In a single-channel nonrelativistic potential picture, the 2S hyperfine splitting is given by $M(\psi') - M(\eta'_c) = 32\pi\alpha_s |\Psi(0)|^2 / 9m_c^2$. Normalizing to the observed 1S hyperfine splitting, $M(J/\psi) - M(\eta_c) = 117$ MeV, we would find $M(\psi') - M(\eta'_c) = 67$ MeV, to be compared with the observed 48 ± 5 MeV separation. The 2S induced shifts calculated in Ref. [8] draw ψ' and η'_c closer by 20.9 MeV, substantially improving the agreement between theory and experiment. It is tempting to conclude that the $\psi' - \eta'_c$ splitting reflects the influence of virtual decay channels.

B. CLEO's h_c candidate

Like the η'_c , the spin-singlet $L = 1$ level of charmonium has been an object of desire for three decades. The barrier to observation has been the absence of allowed E1 or M1 transitions from the $J^{PC} = 1^{--}$ states readily formed in e^+e^- annihilations. The 1^1P_1 state holds a special interest, beyond the tidiness that would come from completing the spectrum of narrow states. In the nonrelativistic potential-model descriptions that have provided such a reliable guide to quarkonium spectroscopy, the central potential is generally taken to consist of a Coulomb piece with vector Lorentz structure (arising from one-gluon exchange) plus a confining term with scalar Lorentz structure. For such a potential, the hyperfine splitting between spin-singlet and spin-triplet orbital excitations is very small. A significant deviation from the expectation that $M(1^1P_1) \approx \langle M(1^3P_J) \rangle$ could offer evidence for an unexpected Lorentz structure, or for the importance of effects not included in the nonrelativistic potential-model description.

An earlier observation of $\bar{p}p \rightarrow h_c \rightarrow \pi^0 \eta_c$ near the (1^3P_J) centroid in Fermilab Experiment 760 [21] is not sustained by two additional data runs with $2\times$ and $3\times$ the luminosity in the successor experiment E835 [22,23]. E835 does report a narrow ($\Gamma < 1$ MeV) event excess in the $\bar{p}p \rightarrow h_c \rightarrow \gamma \eta_c$ channel at a mass $M(h_c) = 3525.8 \pm 0.2 \pm 0.2$ MeV [22]. The signal bin contains 13 signal events on a 3-event background, and the signal strength is $\Gamma(h_c \rightarrow \bar{p}p) \mathcal{B}(h_c \rightarrow \gamma \eta_c) \approx 11$ eV.

The CLEO Collaboration has examined 3.08×10^6 $\psi(2S)$ decays, in search of examples of the isospin-violating decay to $\pi^0 h_c$, followed by $\pi^0 \rightarrow \gamma\gamma$ and $h_c \rightarrow \gamma \eta_c$ [2,3]. They find 150 ± 40 signal counts for the inclusive channel, in which η_c is not reconstructed, and 17.5 ± 4.5 signal counts spread over seven hadronic decay channels of η_c , for a combined significance exceeding 5σ .

In the inclusive sample, the angular distribution of photons in the $h_c \rightarrow \gamma \eta_c$ cascade follows the $1 + \cos^2\theta$ pattern characteristic of E1 emission from a spin-1 state. The CLEO experimenters infer the 1^1P_1 mass $M(h_c) = 3524.4 \pm 0.6 \pm 0.4$ MeV, with a product branching fraction $\mathcal{B}(\psi(2S) \rightarrow \pi^0 h_c) \mathcal{B}(h_c \rightarrow \gamma \eta_c) = (4.0 \pm 0.8 \pm 0.7) \times 10^{-4}$.

The 1^1P_1 level lies $1.0 \pm 0.6 \pm 0.4$ MeV below the spin-triplet centroid, $\langle M(1^3P_J) \rangle = 3525.36 \pm 0.06$ MeV [20], consistent with theoretical expectations.

C. Rare decays of $\psi(3770)$

The color-multipole expansion [24–26] yields symmetry relations for hadronic transition rates between charmonium states but does not enable calculations of rates from first principles. By the Wigner-Eckart theorem for E1-E1 transitions, all the $1^3D_J \rightarrow \pi\pi J/\psi$ rates should be equal (for degenerate 3D_J states), so a reliable determination of the rate $\Gamma(\psi(3770) \rightarrow \pi\pi J/\psi)$ is important for anticipating the properties of ψ_2 and ψ_3 . In our survey of B -meson gateways to missing charmonium states [9], we adopted the value $\Gamma(1^3D_1 \rightarrow \pi\pi J/\psi) \approx 45$ keV.

The CLEO Collaboration has just reported the first high-significance (11.6σ) observation of the decay $\psi(3770) \rightarrow \pi^+ \pi^- J/\psi$ [27]. Their measured branching fraction, $\mathcal{B}(\psi(3770) \rightarrow \pi^+ \pi^- J/\psi) = (1.89 \pm 0.20 \pm 0.20) \times 10^{-3}$, corresponds to a partial width $\Gamma(1^3D_1 \rightarrow \pi^+ \pi^- J/\psi) \approx (45 \pm 9)$ keV. [The CLEO rate is consistent with, but much more precise than, the Beijing Spectrometer observation [28], $\mathcal{B}(\psi(3770) \rightarrow \pi^+ \pi^- J/\psi) = (3.4 \pm 1.4 \pm 0.9) \times 10^{-3}$.] A less significant (3.4σ) observation of the decay $\psi(3770) \rightarrow \pi^0 \pi^0 J/\psi$ is consistent with the expectation that the $\pi^0 \pi^0 J/\psi$ rate should be half the $\pi^+ \pi^- J/\psi$ rate. Accordingly, we shall take $\Gamma(1^3D_J \rightarrow \pi\pi J/\psi) = (68 \pm 15)$ keV as an improved estimate of the dipion decay rates of the ψ_2 and ψ_3 . The increase from our earlier estimate does not alter the expectation that the most prominent decay of the 1^3D_2 state should be $\psi_2 \rightarrow \gamma \chi_{c1}$.

CLEO has also searched for rare radiative decays of $\psi(3770)$, reporting the preliminary values $\Gamma(\psi(3770) \rightarrow \gamma \chi_{c1}) = (78 \pm 19)$ keV and $\Gamma(\psi(3770) \rightarrow \gamma \chi_{c2}) < 20$ keV [29]. These observations are in line with expectations ($\Gamma(1^3D_1 \rightarrow \gamma \chi_{c1}) \approx 59$ keV and $\Gamma(1^3D_1 \rightarrow \gamma \chi_{c2}) \approx 4$ keV [8]) and give us no reason to question the estimated E1 transition rates for the other 1D levels (see Sec. III D).

D. Properties of $X(3782)$

As the best studied of the new $c\bar{c}$ -associated states, $X(3782)$ has been subjected to a broad range of diagnostic tests. Upon discovery, $X(3782)$ seemed a likely—though somewhat heavy—candidate for ψ_2 (or perhaps ψ_3), but the expected radiative transitions to χ_c states have never been seen. For a state that lies approximately 50 MeV

above charm threshold, the narrow width [$\Gamma(X(3872)) < 2.3$ MeV] [4] and the absence of a $D\bar{D}$ signal [30] suggest unnatural parity $P = (-1)^{J+1}$. The *BABAR* Collaboration has set limits on the existence of a charged partner [31]. In 1.96-TeV $\bar{p}p$ collisions, the production characteristics of $X(3872)$ are similar to those of $\psi(2S)$ [6]. CDF has determined the fraction of $X(3872)$ arising from B decays as $16.9 \pm 4.9 \pm 2.0\%$ [32].

The $\pi\pi$ mass spectrum favors high dipion masses [33], suggesting a $J/\psi\rho$ decay that would be incompatible with the identification of $X(3872) \rightarrow \pi^+\pi^-J/\psi$ as the strong decay of a pure isoscalar state. See, however, the interesting discussion of alternative interpretations in Ref. [34]. Suzuki has suggested [35] that the ρ -like behavior of the $\pi^+\pi^-$ mass spectrum in these decays may result from a dominant decay to $\omega J/\psi$ slightly off mass shell and the small (isospin breaking) ω - ρ mixing. In this case the $X(3872)$ could be an isoscalar state as expected in a charmonium interpretation.

Observing—or limiting—the $\pi^0\pi^0J/\psi$ decay remains an important goal [10]. An observed $J/\psi\pi^+\pi^-\pi^0$ decay suggests an appreciable transition rate to $J/\psi\omega$ [36]. Belle’s 4.4- σ observation of the decay $X(3872) \rightarrow J/\psi\gamma$ [36] determines $C = +$, opposite to the charge-conjugation of the leading charmonium candidates. Finally, an analysis of angular distributions [37] supports the assignment $J^{PC} = 1^{++}$ [38], but the mass of $X(3872)$ is too low to be gracefully identified with the 2^3P_1 charmonium state, especially if $Z(3931)$ (cf. Sec. II E 3) is to be identified as the 2^3P_2 level. The χ'_{c1} also lacks an isospin-allowed $\pi\pi J/\psi$ decay mode and acquires a substantial $D\bar{D}^*$ width if $M(\chi'_{c1}) > M(D^0) + M(D^{*0})$. We shall examine this hypothesis further in Sec. IV B 2.

If $X(3872)$ is not a charmonium level, what might it be [39]? Three interpretations take the near coincidence of the new state’s mass and the $D^0\bar{D}^{*0}$ to be a decisive clue: a s -wave cusp at $D^0\bar{D}^{*0}$ threshold [40], a $D^0\bar{D}^{*0}$ “molecule” bound by pion exchange [41–44], and a diquark-antidiquark “tetraquark” state $[cq][\bar{c}\bar{q}]$ [45,46]. According to a different four-quark interpretation, $X(3872)$ is a $c\bar{c}q\bar{q}$ state organized by the chromomagnetic (color-hyperfine) interaction into a $(c\bar{c})_8-(q\bar{q})_8$ pair [47].

What distinctive predictions might allow us to put these interpretations to the test? On the threshold enhancement interpretation, we should expect bumps at many thresholds, but no radial or orbital excitations. If pion exchange is decisive, then there should be no analogue molecule at $D_s\bar{D}_s^*$ threshold. The tetraquark interpretation suggests that $X(3872)$ should be split into two levels, because $[cu][\bar{c}\bar{u}]$ and $[cd][\bar{c}\bar{d}]$ would be displaced by about 7 MeV. A first experimental test by the *BABAR* Collaboration is inconclusive [16]. In 61.2 ± 15.3 events that fit the hypothesis $B^- \rightarrow K^- X(3872)$, they determine a mass of $3871.3 \pm 0.6 \pm 0.1$ MeV, whereas 8.3 ± 4.5 $B^0 \rightarrow K^0 X(3872)$ events yield $3868.6 \pm 1.2 \pm 0.2$ MeV.

The mass difference, $2.7 \pm 1.3 \pm 0.2$ MeV, does not yet distinguish between one X and two. If diquarks are useful dynamical objects, there should be a sequence of excited states as well. On the color-hyperfine $c\bar{c}q\bar{q}$ interpretation, the only analogous level should be a $(b\bar{b})_8-(q\bar{q})_8$ state near $B\bar{B}^*$ threshold.

What if the $D^0\bar{D}^{*0}$ threshold is not the decisive element? Hybrid $c\bar{c}$ -gluon states might appear in the charmonium spectrum [48]. The mass and 1^{++} quantum numbers of $X(3872)$ do not match lattice-QCD expectations [49–51]. The valence gluon in the hybrid charmonium wave function leads to speculation that the $\eta J/\psi$ decay mode might be quite prominent. The *BABAR* experiment [52] has found no sign of $X(3872) \rightarrow \eta J/\psi$. More generally, it is plausible that the gluonic degrees of freedom should manifest themselves as “vibrational states” in the charmonium spectrum [53,54]. While theoretical estimates of the spectrum of string-vibration modes do not reproduce the characteristics of $X(3872)$, we should be alert to the appearance of such states elsewhere.

E. Evidence for states beyond $X(3872)$

The other new states associated with charmonium require confirmation and elaboration. For the moment, experiments have identified four distinct candidates.

1. $Y(3940)$

Exploring the $J/\psi\omega$ mass spectrum in decays $B \rightarrow KJ/\psi\omega$, the Belle Collaboration observed an enhancement of 58 ± 11 events near threshold [12]. Treated as an s -wave resonance, this state, named $Y(3940)$, has a mass $M(Y) = 3943 \pm 11 \pm 13$ MeV and a total width $\Gamma = 87 \pm 22 \pm 26$ MeV. The mass of this object lies well above DD^* threshold, so if $Y(3940)$ is a charmonium state, it would be expected to decay dominantly into $D\bar{D}$ or $D\bar{D}^*$. A small $J/\psi\omega$ decay rate would complicate the interpretation of the product branching fraction, $\mathcal{B}(B \rightarrow KY(3940))\mathcal{B}(Y(3940) \rightarrow J/\psi\omega) = (7.1 \pm 1.3 \pm 3.1) \times 10^{-5}$. For comparison, the branching fractions for the decays $B^+ \rightarrow K^+(c\bar{c})$, with $(c\bar{c}) = \eta_c, J/\psi, \chi_{c0}, \chi_{c1}, \psi'$, are between $6\text{--}10 \times 10^{-4}$ [20]. This suggests a branching ratio of about 10% for $Y(3940) \rightarrow \omega J/\psi$ if $Y(3940)$ is a conventional charmonium state. In contrast, a $c\bar{c}$ -gluon hybrid state might decay preferentially into J/ψ or ψ' plus light hadrons [55,56]. To settle the identity of $Y(3940)$ will require confirming that it is a single state and distinguishing it from the $X(3940)$, to which we now turn.

2. $X(3940)$

The Belle [17,57] and *BABAR* collaborations [58] have observed copious double charmonium production in e^+e^- annihilations, with strong signals for $J/\psi\eta_c, J/\psi\chi_{c0}$, and $J/\psi\eta'_c$. Searching in the region above $D\bar{D}$ threshold, Belle

has observed a new peak at $3943 \pm 6 \pm 6$ MeV, with a width $\Gamma < 52$ MeV at 90% C.L. [13].

The new structure, given the temporary name $X(3940)$, is seen to decay into $D\bar{D}^*$, with a branching fraction $\mathcal{B}(X(3940) \rightarrow D\bar{D}^*) = 0.96^{+0.45}_{-0.32} \pm 0.22$. The absence of any signal in the $D\bar{D}$ channel (for which the branching fraction is < 0.41 at 90% C.L.) suggests that $X(3940)$ is an unnatural parity state. Its properties roughly match those expected for $\eta_c(3S)$, and we shall examine that hypothesis further in Sec. IVA.

3. Z(3930)

The Belle Collaboration has examined the $D\bar{D}$ invariant-mass distribution in $\gamma\gamma$ -fusion events in which the transverse momentum of the $D\bar{D}$ pair is small. A narrow peak of 64 ± 18 events appears at $M(D\bar{D}) = 3929 \pm 5 \pm 2$ MeV [14]. The state, provisionally named $Z(3930)$, has a total width $\Gamma(Z(3930)) = 29 \pm 10 \pm 2$ MeV, and $\Gamma(Z(3930) \rightarrow \gamma\gamma)\mathcal{B}(Z(3930) \rightarrow D\bar{D}) = 0.18 \pm 0.05 \pm 0.03$ keV, assuming $J = 2$. The (helicity) angular distribution strongly prefers $\sin^4\theta^*$, which corresponds to a spin-2 resonance, over the flat angular distribution characteristic of spin-0. Belle accordingly proposes to identify $Z(3930)$ as the 2^3P_2 χ'_{c2} . The measured properties are in reasonable accord with those anticipated in Ref. [8]; we probe the 2^3P_2 assignment further in Sec. IV B 1.

4. Y(4260)

In a study of initial-state radiation events, $e^+e^- \rightarrow (\gamma)\pi^+\pi^-J/\psi$, the BABAR Collaboration has observed an accumulation of events near 4260 MeV in the $\pi^+\pi^-J/\psi$ invariant-mass distribution [15]. The excess of 125 ± 23 events can be characterized as a single $J^{PC} = 1^{--}$ resonance with mass $4259 \pm 8^{+2}_{-6}$ MeV and total width $\Gamma(Y(4260)) = 88 \pm 23^{+6}_{-4}$ MeV, but a more complicated structure has not been ruled out. It is perhaps significant that $Y(4260)$ lies near the $D_s^{*+}\bar{D}_s^{*-}$ threshold at 4224 MeV. BABAR also reports a 3.1σ signal for $Y(4260)$ in exclusive $B^\pm \rightarrow K^\pm\pi^+\pi^-J/\psi$ decays [16]. An excess of 128 ± 42 signal events corresponds to a product branching fraction $\mathcal{B}(B^- \rightarrow K^-Y(4260))\mathcal{B}(Y(4260) \rightarrow \pi^+\pi^-J/\psi) = (2.0 \pm 0.7 \pm 0.2) \times 10^{-5}$.

The new state has variously been interpreted as $\psi(4S)$, a $c\bar{c}g$ hybrid state [56,59,60], and the radial excitation of a diquark-antidiquark state identified with $X(3872)$ [46]. Curiously, the $\pi^+\pi^-J/\psi$ enhancement occurs in the neighborhood of a local minimum in the cross section for electron-positron annihilation into hadrons. We will have more to say about possible interpretations in Sec. IV C.

III. STRONG DYNAMICS NEAR THRESHOLD

Near the threshold for open heavy-flavor pair production, light-quark pairs induce significant nonperturbative contributions to the masses, wave functions, and decay

properties of physical $Q\bar{Q}$ states. Lattice QCD calculations, once extended into the flavor-threshold region, should provide firm theoretical predictions. At present, only a phenomenological approach can offer a detailed description of these effects.

The effects of light-quark pairs can be described by coupling the potential-model $Q\bar{Q}$ states to nearby physical multibody states. In this threshold picture, the strong interactions are broken into sectors defined by the number of valence quarks. We decompose the full Hamiltonian \mathcal{H} as

$$\mathcal{H} = \sum_n \mathcal{H}_n + \mathcal{H}_I, \quad (1)$$

where \mathcal{H}_n is the Hamiltonian that governs the $(c\bar{c}) + n$ -light-quark sector, and \mathcal{H}_I is the interaction that couples the various sectors.

The dynamics of the $Q\bar{Q}$ states (with no valence light quarks, q) is described by the interaction \mathcal{H}_0 . In principle, excited $Q\bar{Q}$ states with valence or vibrational gluonic degrees of freedom also would be contained in the spectrum of \mathcal{H}_0 . In practice, a simple nonrelativistic potential model is used to determine the properties of the bound states in this sector.

The two-meson sector $Q\bar{q} + q\bar{Q}$ is described by the Hamiltonian \mathcal{H}_2 . As a first approximation, we shall assume \mathcal{H}_2 to be represented by the low-lying spectrum of two free heavy-light mesons. The physical situation is more complex. At large separation between the two mesons the interactions are dominated by t -channel pion exchanges, when they are allowed. For states very near threshold such as $X(3872)$, such pion exchange in attractive channels might have significant effects on properties of the physical states [61]. At somewhat shorter distances, more complicated interactions exist and new bound states might arise, e.g. molecular states [41–44,62–64]. Furthermore, at small $Q\bar{Q}$ separation the $Q\bar{Q} + q\bar{q}$ sector may contribute significantly to \mathcal{H}_2 . In particular, as Swanson has emphasized [65], the $\rho J/\psi$ and $\omega J/\psi$ thresholds lie in the $D\bar{D}$ threshold region. The main landmarks throughout the region we consider are shown in Table I.

Because current mastery of nonperturbative quantum chromodynamics does not suffice to derive a realistic description of the interactions that link the $Q\bar{Q}$ and $Q\bar{q} + q\bar{Q}$ sectors, we must resort to a phenomenological *ansatz* for \mathcal{H}_I . Following our earlier work [8], we consider here the Cornell coupled-channel (C^3) model [66–68] for the creation of $q\bar{q}$ pairs. A brief discussion of various other models for \mathcal{H}_I is contained in the Quarkonium Working Group's CERN Yellow Report [69]. The open-charm threshold region occupies our interest in this study. However, analogous effects are present in the $b\bar{b}$ states near $B\bar{B}$ threshold and $c\bar{b}$ states near DB threshold. A detailed comparison of different heavy-quark systems could provide valuable insight into the correct form for the coupling to light-quark pairs.

TABLE I. Thresholds for decay into open-charm and nearby hidden-charm thresholds.

Channel	Threshold energy (MeV)
$D^0\bar{D}^0$	3729.4
D^+D^-	3738.8
$D^0\bar{D}^{*0}$ or $D^{*0}\bar{D}^0$	3871.2
$\rho^0 J/\psi$	3872.7
$D^\pm D^{*\mp}$	3879.5
$\omega^0 J/\psi$	3879.6
$D_s^+ D_s^-$	3936.2
$D^{*0}\bar{D}^{*0}$	4013.6
$D^{*+} D^{*-}$	4020.2
$\eta' J/\psi$	4054.7
$f^0 J/\psi$	≈ 4077
$D_s^+ \bar{D}_s^{*-}$ or $D_s^{*+} \bar{D}_s^-$	4080.0
$a^0 J/\psi$	4081.6
$\varphi^0 J/\psi$	4116.4
$D_s^{*+} D_s^{*-}$	4223.8
$\Lambda_c \bar{\Lambda}_c$	4569.8

The C^3 formalism generalizes the $c\bar{c}$ model without introducing new parameters, writing the interaction Hamiltonian in second-quantized form as

$$\mathcal{H}_I = \frac{3}{8} \sum_{a=1}^8 \int : \rho_a(\mathbf{r}) V(\mathbf{r} - \mathbf{r}') \rho_a(\mathbf{r}') : d^3 r d^3 r', \quad (2)$$

where V is the charmonium potential and $\rho_a(\mathbf{r}) = \frac{1}{2} \psi^\dagger(\mathbf{r}) \lambda_a \psi(\mathbf{r})$ is the color current density, with ψ the quark field operator and λ_a the octet of SU(3) matrices. To generate the relevant interactions, ψ is expanded in creation and annihilation operators (for charm, up, down, and strange quarks), but transitions from two mesons to three mesons and all transitions that violate the Zweig rule are omitted. It is a good approximation to neglect all effects of the Coulomb piece of the potential in (2). This simple model for the coupling of charmonium to charmed-meson decay channels gives a qualitative understanding of the structures observed above threshold while preserving the successes of the single-channel $c\bar{c}$ analysis below threshold [67,68].

A. Mass shifts

In the presence of coupling to two-light-quark decay channels, the mass ω of the quarkonium state Ψ is defined by the eigenvalue equation

$$[\mathcal{H}_0 + \mathcal{H}_2 + \mathcal{H}_I] \Psi = \omega \Psi. \quad (3)$$

Above the flavor threshold, ω is a complex eigenvalue.

The basic coupled-channel interaction \mathcal{H}_I given by (2) is independent of the heavy quark's spin, but the hyperfine splittings of D and D^* , D_s and D_s^* , induce spin-dependent forces that affect the charmonium states. These spin-dependent forces give rise to S-D mixing that contributes

to the electronic widths of 3D_1 states and induces additional spin splitting among the physical states.

The masses that result from the full coupled-channel analysis are shown in the second column of Table II, which revises and extends our previously published results [8]. The new version presented here includes the 3S levels and takes account of Belle's evidence [14] for $Z(3930)$, interpreted as a 2^3P_2 state (cf. Sec. II E 3). As in our earlier analysis, the parameters of the potential-model sector governed by \mathcal{H}_0 must be readjusted to fit the physical masses, ω , to the observed experimental values. The centroids of the 1D and 2P spin-triplet masses are pegged to the observed masses of 1^3D_1 [$\psi(3770)$] and 2^3P_2 [$Z(3930)$], respectively. The assumed spin splittings in the single-channel potential model are shown in the penultimate column and the induced coupled-channel spin splittings for initially unsplit multiplets are presented in the rightmost column of Table II. The shifts induced in the low-

TABLE II. Charmonium spectrum, including the influence of open-charm channels. All masses are in MeV. The penultimate column holds an estimate of the spin splitting due to tensor and spin-orbit forces in a single-channel potential model. The last column gives the spin splitting induced by communication with open-charm states, for an initially unsplit multiplet.

State	Mass	Centroid	Splitting (potential)	Splitting (induced)
1^1S_0	2979.9 ^a	3067.6 ^b	-90.5 ^c	+2.8
1^3S_1	3096.9 ^a		+30.2 ^c	-0.9
1^3P_0	3415.3 ^a	3525.3 ^c	-114.9 ^e	+5.9
1^3P_1	3510.5 ^a		-11.6 ^e	-2.0
1^1P_1	3524.4 ^f		+0.6 ^e	+0.5
1^3P_2	3556.2 ^a		+31.9 ^e	-0.3
2^1S_0	3638 ^a	3674 ^b	-50.1 ^e	+15.7
2^3S_1	3686.0 ^a		+16.7 ^e	-5.2
1^3D_1	3769.9 ^a	(3815) ^d	-40	-39.9
1^3D_2	3830.6		0	-2.7
1^1D_2	3838.0		0	+4.2
1^3D_3	3868.3		+20	+19.0
2^3P_0	3881.4	(3922) ^d	-90	+27.9
2^3P_1	3920.5		-8	+6.7
2^1P_1	3919.0		0	-5.4
2^3P_2	3931 ^g		+25	-9.6
3^1S_0	3943 ^h	(4015)	-66 ^e	-3.1
3^3S_1	4040 ^a	(4015)	+22 ^e	+1.0

^aObserved mass, from *Review of Particle Physics*, Ref. [20].

^bInput to potential determination.

^cObserved 1^3P_J centroid.

^dComputed centroid.

^eRequired to reproduce observed masses.

^fObserved mass from CLEO [3].

^gObserved mass from Belle [14].

^hObserved mass from Belle [13].

ⁱObserved 3S centroid.

lying 1S and 1P levels are small. For all the other states, coupled-channel effects are noticeable and interesting.

An important consequence of coupling to the open-charm threshold is that the ψ' receives a downward shift through its communication with the nearby $D\bar{D}$ channel; the unnatural parity η'_c does not couple to $D\bar{D}$, and so is not depressed in the same degree. This effect is implicitly present in the early Cornell papers [67,68], but the shift of spin-singlet states was not calculated there. The first explicit mention—and the first calculation—of the unequal effects on the masses of the 2S hyperfine partners is due to Martin and Richard [70]. In the framework of the C^3 model, we found [8,9] (cf. Table II) that the induced shifts draw ψ' and η'_c closer by 20.9 MeV, substantially improving the agreement between theory and experiment. This suggests that the ψ' - η'_c splitting reflects the influence of virtual decay channels. In the case of the 3S system, both the 3^1S_0 η''_c and the 3^3S_1 $\psi(4040)$ communicate with open decay channels, and the C^3 model leads to a modest 9 MeV increase in the interval between them, as seen in Table II.

B. Mixing and properties of physical states

The physical states are not pure potential-model eigenstates but include components with two virtual (real, above threshold) open-flavor meson states. Separating the physical state Ψ into $Q\bar{Q}$ (Ψ_0) and two-charmed-meson components (Ψ_2), the resulting decomposition of \mathcal{H} by sector leads to an effective Hamiltonian for the $Q\bar{Q}$ sector given by

$$\left[\mathcal{H}_0 + \mathcal{H}_I^\dagger \frac{1}{\omega - \mathcal{H}_2 + i\epsilon} \mathcal{H}_I \right] \Psi_0 = \omega \Psi_0. \quad (4)$$

Solving Eq. (4) in the $Q\bar{Q}$ sector determines the mixing among the potential-model states and the coupling to decay channels. Computational procedures for the C^3 model based on the coupling Hamiltonian (2) have been described in detail elsewhere [8,67,68]. Even above threshold for strong decays, the coupled-channel Hamiltonian approach (4) allows a definition of the mass and width of the resonances in terms of the complex eigenvalues and a decomposition of the state into the $c\bar{c}$ and $D\bar{D}$ components via the associated eigenvector. Of course, the width and mass so defined will differ somewhat from the resonance mass and width inferred from the observed enhancement in any particular open-charm–meson-pair channel.

The two-meson contributions to the wave functions of the low-lying $c\bar{c}$ states are shown in Table III for the C^3 model. The overall probability for the physical state to be in what we have called the Ψ_0 ($c\bar{c}$) sector, denoted $Z_{c\bar{c}}$, decreases as charm threshold is approached. For states above threshold the mixing coefficients become complex, as shown in Table IV. Configuration mixing effects modify radiative transition rates [8,71,72], in addition to their influence on S-D mixing and spin splittings we have already mentioned.

TABLE III. Wave function fractions (in percent) in the Ψ_0 ($c\bar{c}$) and Ψ_2 [$D^{(*)}\bar{D}^{(*)}$] sectors for near-threshold states.

State	Ψ_0 fraction $Z_{c\bar{c}}$	Ψ_2 fraction			
		$D\bar{D}$	$D\bar{D}^* + D^*\bar{D}$	$D^*\bar{D}^*$	
1^3D_1	96.83	<i>u</i>	0.14	0.46	0.67
		<i>d</i>	0.14	0.46	0.66
		<i>s</i>	0.07	0.23	0.34
1^3D_2	61.10	<i>u</i>	0.00	15.10	3.30
		<i>d</i>	0.00	13.94	3.21
		<i>s</i>	0.00	2.38	0.96
1^1D_2	63.36	<i>u</i>	0.00	12.33	4.88
		<i>d</i>	0.00	11.38	4.74
		<i>s</i>	0.00	2.00	1.31
1^3D_3	50.06	<i>u</i>	16.51	1.59	7.47
		<i>d</i>	13.17	1.54	7.20
		<i>s</i>	0.25	0.43	1.77
2^3P_0	50.03	<i>u</i>	16.48	0.00	5.23
		<i>d</i>	17.74	0.00	5.04
		<i>s</i>	4.41	0.00	1.06
2^1P_1	50.04	<i>u</i>	0.00	19.40	4.95
		<i>d</i>	0.00	18.73	4.68
		<i>s</i>	0.00	1.43	0.78
2^3P_1	50.06	<i>u</i>	0.00	20.82	3.10
		<i>d</i>	0.00	20.41	2.99
		<i>s</i>	0.00	2.00	0.63
2^3P_2	49.95	<i>u</i>	4.47	12.80	7.74
		<i>d</i>	4.32	11.47	7.17
		<i>s</i>	0.24	0.87	0.97
3^1S_0	50.05	<i>u</i>	0.00	20.78	4.02
		<i>d</i>	0.00	19.82	3.78
		<i>s</i>	0.00	1.01	0.55
3^3S_1	50.04	<i>u</i>	1.42	10.12	11.86
		<i>d</i>	1.45	10.24	11.24
		<i>s</i>	0.98	1.58	1.08
2^3D_1	71.80	<i>u</i>	4.43	4.16	4.49
		<i>d</i>	3.94	3.98	4.38
		<i>s</i>	0.55	0.96	1.31

C. Zweig-allowed strong decays

Once the mass of a resonance is given, the C^3 formalism yields reasonable predictions for the other resonance properties. We present in Table V our estimates of the strong decay rates for all the *s*-, *p*-, and *d*-wave charmonium levels that populate the threshold region below 4200 MeV, together with what is known from experiment. No new experimental information has come to light about $L \geq 3$ levels; the predictions given in Ref. [8] remain current.

The 1^3D_1 state $\psi''(3770)$, which lies some 40 MeV above charm threshold, calibrates the reasonableness of our calculated widths. As we noted in Ref. [8], our value

TABLE IV. Charmonium content of states near $c\bar{c}$ threshold. The wave function Ψ reflects mixing induced through communication with open-charm channels. Unmixed potential-model eigenstates are denoted by $|n^{2s+1}L_J\rangle$. The coefficient of the dominant unmixed state is chosen real and positive. Physical states are evaluated at masses given in Table II.

State	Principal $\Psi_0(c\bar{c})$ components
$\Psi(1^3D_1)$	$= 0.10e^{+0.59i\pi} 2S\rangle + 0.01e^{+0.81i\pi} 3S\rangle$ $+ 0.69 1D\rangle + 0.10e^{+0.86i\pi} 2D\rangle$
$\Psi(1^3D_2)$	$= 0.77 1D\rangle - 0.10 2D\rangle - 0.02 3D\rangle$
$\Psi(1^1D_2)$	$= 0.79 1D\rangle - 0.10 2D\rangle - 0.02 3D\rangle$
$\Psi(1^3D_3)$	$= 0.70 1D\rangle - 0.09 2D\rangle + 0.02e^{-0.98i\pi} 3D\rangle$
$\Psi(2^3P_0)$	$= 0.11e^{-0.38i\pi} 1P\rangle + 0.70 2P\rangle + 0.03e^{+0.56i\pi} 3P\rangle$
$\Psi(2^1P_1)$	$= 0.18e^{-0.19i\pi} 1P\rangle + 0.68 2P\rangle + 0.07e^{+0.77i\pi} 3P\rangle$
$\Psi(2^3P_1)$	$= 0.18e^{-0.27i\pi} 1P\rangle + 0.68 2P\rangle + 0.07e^{+0.69i\pi} 3P\rangle$
$\Psi(2^3P_2)$	$= 0.18e^{-0.09i\pi} 1P\rangle + 0.66 2P\rangle + 0.07e^{+0.85i\pi} 3P\rangle$
$\Psi(3^1S_0)$	$= 0.02e^{-0.06i\pi} 1S\rangle + 0.20e^{-0.18i\pi} 2S\rangle + 0.68 3S\rangle$ $+ 0.05e^{+0.67i\pi} 4S\rangle$
$\Psi(3^3S_1)$	$= 0.02e^{-0.05i\pi} 1S\rangle + 0.19e^{-0.30i\pi} 2S\rangle + 0.67 3S\rangle$ $+ 0.07e^{+0.54i\pi} 4S\rangle$ $+ 0.04e^{+0.59i\pi} 1D\rangle + 0.04e^{+0.59i\pi} 2D\rangle$
$\Psi(2^3D_1)$	$= 0.02e^{+0.60i\pi} 2S\rangle + 0.03e^{-0.71i\pi} 3S\rangle$ $+ 0.14e^{-0.50i\pi} 1D\rangle + 0.69 2D\rangle$

of 20.1 MeV is in excellent agreement with the world average, $\Gamma(\psi(3770)) = 23.6 \pm 2.7$ MeV [20].

The results presented here differ in two respects from those of Ref. [8]. First, the χ'_{c2} and η'_c masses have been fixed, if only provisionally, by experiment. This results in shifts of the masses and properties of all the 2P and 3S states as shown in Tables II, V, and VI. Second, the present approach allows a more detailed extraction of the composition of the charmonium states above threshold. These results are shown in Tables III and IV.

Along with the current PDG values for the total widths of higher $1^{--} c\bar{c}$ resonances, we show in Table V a reanalysis of the existing experimental data by Seth [73].

The natural-parity 1^3D_3 state can decay into $D\bar{D}$, but its f -wave decay is suppressed by the centrifugal barrier factor. Thus the 1^3D_3 may be discovered as a narrow $D\bar{D}$ resonance up to a mass of about 4000 MeV.

Barnes, Godfrey, and Swanson [11] have recently reported extensive calculations of decay widths of higher charmonium states in the framework of the 3P_0 model for quark-pair production. [Shortcomings of both the C^3 and 3P_0 models are assessed in Ref. [69]. Detailed comparisons (e.g. Ackleh, Barnes, and Swanson [74]) between various light-quark pair creation models are highly desirable.] Unlike the analysis presented here, their calculation does not resum the effects of coupling to decay channels. The general scale of resulting decay rates is similar to those displayed in Table V. For example, Barnes *et al.* determine $\Gamma(3^3S_1) = 80$ MeV and $\Gamma(2^3D_1) = 74$ MeV.

TABLE V. Open-charm strong decay modes of the charmonium states near threshold. The theoretical widths using the C^3 model [8] are shown.

State	$n^{2s+1}L_J$	Mode	Decay width (MeV)	
			Experiment	Computed
$\psi(3770)$	1^3D_1	$D^0\bar{D}^0$		11.8
		D^+D^-		8.3
		total	23.6 ± 2.7^b	20.1
$\psi(3868)$	1^3D_3	$D\bar{D}$		0.82
		total		0.82
$\chi'_{c0}(3881)$	2^3P_0	$D\bar{D}$		61.5
		total		61.5
$h'_{c1}(3919)$	2^1P_1	$D\bar{D}^*$		59.8
		total		59.8
$\chi'_{c1}(3920)$	2^3P_1	$D\bar{D}^*$		81.0
		total		81.0
$\chi'_{c2}(3931)$	2^3P_2	$D\bar{D}$		21.5
		$D\bar{D}^*$		7.1
		total	$29 \pm 10(\text{stat}) \pm 2(\text{sys})^d$	28.6
$\eta'_c(3943)$	3^1S_0	$D\bar{D}^*$		49.8
		total	$< 52^e$	49.8
$\psi(4040)$	3^3S_1	$D\bar{D}$		0.1
		$D\bar{D}^*$		33.0
		$D_s\bar{D}_s$		8.0
		$D_s^*\bar{D}_s^*$		33.0
		total	52 ± 10^b 88 ± 5^c	74.0
$\psi(4159)$	2^3D_1	$D\bar{D}$		3.2
		$D\bar{D}^*$		6.9
		$D_s^*\bar{D}_s^*$		41.9
		$D_s\bar{D}_s$		5.6
		$D_s\bar{D}_s^*$		11.0
total	78 ± 20^b 107 ± 8^c	69.2		

^aComputed from CLEO branching fractions [13].

^bReview of Particle Physics [20].

^cReanalysis by Seth [73].

^dBelle [14].

^eBelle [13].

D. Radiative transitions

As Tables III and IV show, the physical charmonium states are not pure potential-model eigenstates. To compute the E1 radiative transition rates, we must take into account both the standard $(c\bar{c}) \rightarrow (c\bar{c})\gamma$ transitions and the transitions between (virtual) decay channels in the initial and final states. Details of the calculational procedure are given in Sec. IV.B of Ref. [68]. There we also illuminated the differences between single-channel and coupled-channel expectations for the radiative rates.

Our expectations for E1 transition rates among spin-triplet levels are shown in Table VI. Again the observed properties of $\psi(3770)$ confirm the reasonableness of the C^3

TABLE VI. Calculated and observed rates for E1 radiative transitions among charmonium levels. C^3 model rates include the influence of open-charm channels. Photon energies, in MeV, in parentheses.

	Partial width (keV)		
$1^3D_1(3770) \rightarrow$ model	$\chi_{c2}\gamma(208)$ 3.9	$\chi_{c1}\gamma(251)$ 59	$\chi_{c0}\gamma(338)$ 225
CLEO [75]	<40	75 ± 18	<1100
$1^3D_2(3831) \rightarrow$ model	$\chi_{c2}\gamma(266)$ 45	$\chi_{c1}\gamma(308)$ 212	
$1^3D_3(3868) \rightarrow$ model	$\chi_{c2}\gamma(303)$ 286		
$2^3P_0(3881) \rightarrow$ model	$J/\psi\gamma(704)$ 39	$\psi'\gamma(190)$ 17	$1^3D_1\gamma(110)$ 1.6
$2^3P_1(3920) \rightarrow$ model	$1^3D_1\gamma(147)$ 5.2	$1^3D_2\gamma(86)$ 2.6	
$2^3P_1(3920) \rightarrow$ model	$J/\psi\gamma(737)$ 15	$\psi'\gamma(227)$ 75	
$2^3P_2(3931) \rightarrow$ model	$1^3D_1\gamma(157)$ 0.4	$1^3D_2\gamma(95)$ 3.0	$1^3D_3\gamma(62)$ 3.6
$2^3P_2(3931) \rightarrow$ model	$J/\psi\gamma(775)$ 14	$\psi'\gamma(272)$ 120	
$\psi(4040) \rightarrow$ model	$2^3P_2\gamma(84)$ 18	$2^3P_1\gamma(132)$ 5.4	$2^3P_0\gamma(156)$ 20
$\psi(4040) \rightarrow$ model	$1^3P_2\gamma(456)$ 12	$1^3P_1\gamma(495)$ 0.4	$1^3P_0\gamma(577)$ 0.03

framework. The radiative decay rates for the 2^3P_J and 3^3S_1 levels are calculated at the predicted masses. All these rates are small compared to the expected open-charm decay rates.

IV. IMPLICATIONS FOR NEWFOUND STATES

A. $X(3940)$ as $\eta_c(3S)$

The observation by Belle [13] of a state $X(3940)$ recoiling against the J/ψ system in continuum production at the $Y(4S)$ region fits the general behavior expected for the η_c'' charmonium level. This state is not seen to decay into $D\bar{D}$ but does decay into $D\bar{D}^*$, suggesting that it has unnatural parity. Figure 1 shows the complex pole position of the η_c'' in the C^3 model as its bare mass is varied in 10-MeV steps. At 3943 MeV, we estimate a $D\bar{D}^*$ width of 50 MeV, which is quite close to the experimental upper bound on the total width, $\Gamma(X(3940)) < 52$ MeV.

If $\psi(4040)$ is assigned to the 3^3S_1 level, it is somewhat problematic to identify $X(3940)$ as its hyperfine partner. We show in Fig. 2 the behavior of the physical mass and width of the triplet 3S state as the bare mass is varied in 10-MeV steps. To reproduce the observed masses, we would require the spin splitting in the charmonium sector to be 88 MeV, which is considerably larger than the 2S splitting, and larger than expected in naïve potential models.

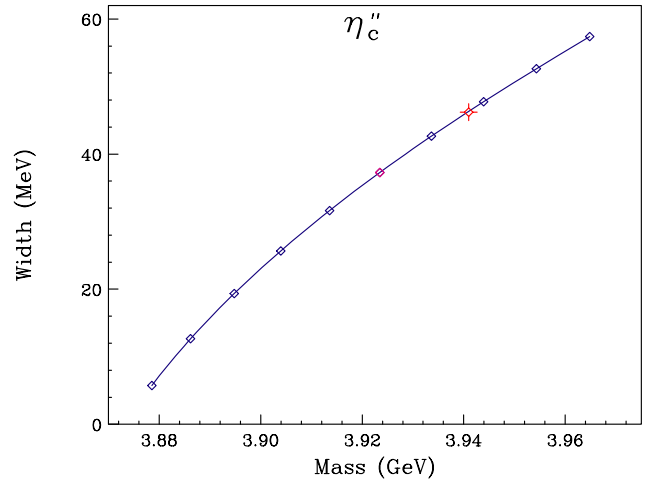


FIG. 1 (color online). Variation of the η_c'' width with mass in the C^3 model. The physical mass of the $X(3940)$ is denoted by a crossed dot.

If, for the moment, we take the existence, mass, and unnatural parity of $X(3940)$ as well established, then two possible sources of the discrepancy deserve further investigation.

First, it is difficult to determine the true pole position for the 3^3S_1 state from measurements of the step in $R_{c\bar{c}} \equiv \sigma(e^+e^- \rightarrow \text{hadrons})/\sigma(e^+e^- \rightarrow \mu^+\mu^-)$ [73]. The resonance decay widths are determined from fitting measurements of ΔR in e^+e^- annihilation to a model for each resonance including radiative corrections. This whole procedure is complicated by its dependence on the resonance shape, i.e., the expected non-Breit-Wigner nature of the partial widths for radially excited resonances. It may be more useful to produce a model of ΔR for direct compari-

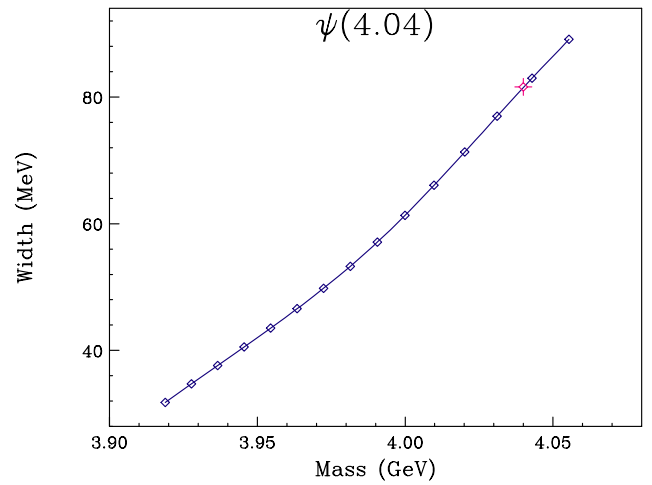


FIG. 2 (color online). Width of the 3^3S_1 state as a function of its mass. The physical mass of the $\psi(4040)$ is denoted by a crossed dot.

son with data. Greater resolving power between models is possible if the contribution from each individual open heavy-flavor final state is separately reported.

For the C^3 model, the structure of $\Delta R(c\bar{c})$ in the threshold region was studied in the original Cornell group works [66–68] and later extended to the $\Delta R(b\bar{b})$ in the threshold region [76]. The structure of $\Delta R(c\bar{c})$ and $\Delta R(b\bar{b})$ has been studied also in 3P_0 models of quark-pair creation [77]. There are also some attempts to compare the different models [78,79].

Second, thresholds corresponding to a s -wave plus a p -wave charmed meson are nearby. Unlike the two s -wave charm meson channels, which are p -wave decays for the $3S$ states, these are s -wave decays and thus have stronger threshold effects. In particular the lowest mass channel $D(J=0; j_i^p=1/2^-)D(J=0; j_i^p=1/2^+)$ couples to the ${}^3S_1 \eta_c''$ state but not the ${}^3S_1 \psi(4040)$ state. This will increase the induced spin splitting (see Table II, column 5) between the states. Thus the observed $\psi'' - \eta_c''$ separation will correspond to a smaller potential-model splitting (column 4).

B. The 2P states

1. $Z(3930)$ as χ_{c2}'

Belle has also observed the new state $Z(3930)$ in two-photon production of $D\bar{D}$ pairs [14]. The 2^3P_2 and 2^3P_0 levels are natural charmonium candidates; experiment favors the $J=2$ assignment. In constructing Table II, we adjusted the 2P centroid to give the mass of the $J=2$ state in agreement with observation. At the observed mass, we compute $\Gamma(2^3P_2 \rightarrow D\bar{D}) = 21.5$ MeV and $\Gamma(2^3P_2 \rightarrow D\bar{D}^*) = 7.1$ MeV, in reasonable agreement with experiment (see Table V). We show in Fig. 3 the variation of the 2^3P_2 pole position with bare mass in 10-MeV steps, using Eq. (4) to fully account for finite-width effects.

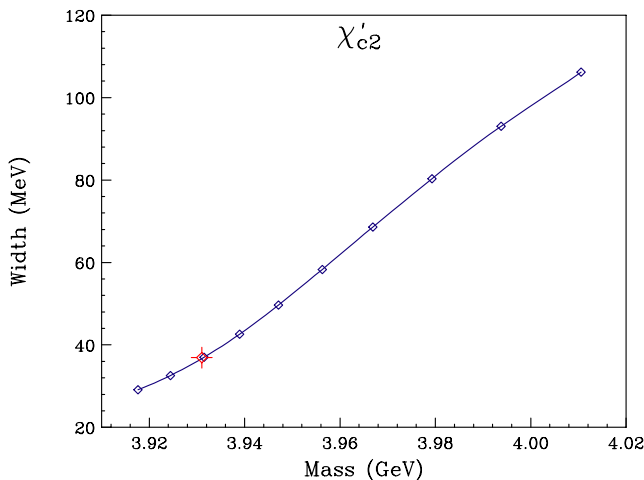


FIG. 3 (color online). Mass dependence of $\Gamma(2^3P_2)$.

2. $X(3872)$ as 2^3P_1

If $X(3872)$ is a 1^{++} state, the unique surviving $c\bar{c}$ candidate would be the 2^3P_1 level [35]. One problem with this interpretation is clear: the expected mass (cf. Table II) is 48 MeV above the observed X mass. If $Z(3930)$ is indeed the 2^3P_2 level, it is very unlikely that its $J=1$ partner should lie at 3872 MeV.

If the mass were not a problem, the 2^3P_1 interpretation would still be difficult to sustain. The E1 radiative transition to $\gamma J/\psi$ is greatly suppressed because of a cancellation between the $c\bar{c}$ and $D\bar{D}^*$ contributions. We obtain 35 and 21 keV for the transitions to J/ψ and ψ' respectively from the $c\bar{c}$ contributions alone. When the effects of the charmed-meson virtual channels are included, the rates change dramatically to 2.4 and 90 keV, respectively. This would make the reported observation of the $\gamma J/\psi$ mode highly unlikely. Of course, within the C^3 model the isospin breaking between $D^0\bar{D}^{*0}$ and D^+D^{*-} virtual states is relatively small. Even if we assume it to be large, so that only the virtual $D^0\bar{D}^{*0}$ component is important, our analysis suggests that a search for the radiative decay to ψ' would be valuable.

Finally, the decay rate of $2^3P_1 \rightarrow D\bar{D}^*$ increases very rapidly above threshold as shown in Fig. 4. Since the total width of $X(3872)$ is less than 2.3 MeV, the possibility that the 2^3P_1 level lies more than 22 keV above the $D^0\bar{D}^{*0}$ threshold is precluded. When the additional partial width Γ_{other} of the 2^3P_1 into other modes (ggg , $\gamma J/\psi$, etc.) is taken into account, the largest tenable mass is lowered to $M(D^0) + M(D^{*0}) - \Gamma_{\text{other}}$. Combining this result with the large ratio of $\Gamma(X(3872) \rightarrow D^0\pi^0\bar{D}^0) \approx 10\Gamma(X(3872) \rightarrow \pi\pi J/\psi)$ reported by Belle [80] renders the 2^3P_1 interpretation very improbable.

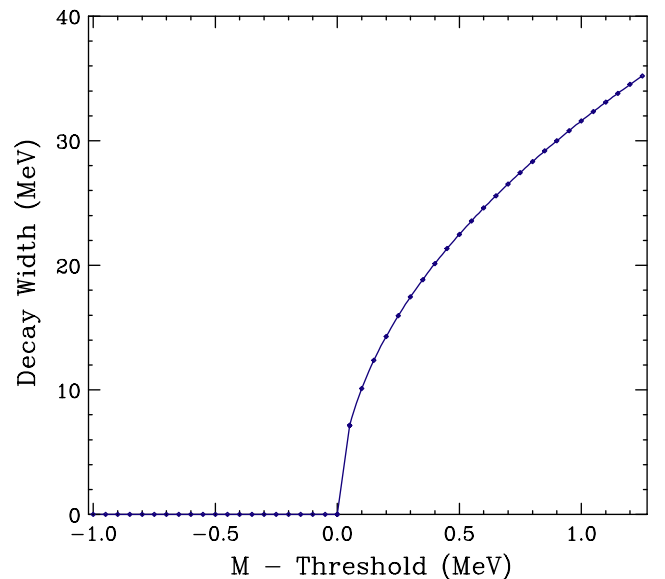


FIG. 4 (color online). Mass dependence of $\Gamma(2^3P_1) \rightarrow D\bar{D}^*$.

C. $Y(4260)$ and other states

In initial-state radiation events, *BABAR* [15] has recently reported a $\pi\pi J/\psi$ resonance, $Y(4260)$, with a width of approximately 88 MeV. This state is hard to assign within the $c\bar{c}$ spectrum. To be directly produced from a virtual photon, it must be a $J^{PC} = 1^{--}$ S or D state. The small contribution to ΔR discourages the 4S interpretation, but leaves open the 2^3D_1 identification. However the C^3 analysis requires that state at 4.16 GeV in order to reproduce the structure of ΔR . The identification of the $Y(4260)$ with the 2^3D_1 state is ruled out in the C^3 model because the partial decay width of the 2D state (at 4260 MeV) into charm meson pairs is 125 MeV. This is not the discovery mode for $Y(4260)$ but exceeds the reported total width. Therefore, this state does not have a conventional charmonium interpretation. One plausible explanation for this state is that it is a hybrid state [56,59]. The lattice calculations of Juge and collaborators [49,51] for the $Q\bar{Q}$ potentials with excited gluonic modes give a lowest multiplet (H_1 in their notation) consisting of a quark spin-singlet 1^{--} state and a spin-triplet set of states (0^{-+} , 1^{-+} , and 2^{-+}). These states would be degenerate in the absence of relativistic spin-dependent mass corrections. If this interpretation were correct, then analogous narrow states would be expected in the $b\bar{b}$ system.

V. SUMMARY

The computed properties of the 2^3P_2 and $3^1S_0 c\bar{c}$ levels are in rough agreement with the $Z(3930)$ and $X(3943)$

states observed at Belle. We await more statistics and confirmation of these results to make a definitive statement on the identification of these states.

It is extremely important to solidify what appears to be known about $X(3872)$, the best studied of the new states, beginning with its 1^{++} quantum numbers. We emphasize the need to confirm the $\gamma J/\psi$ decay mode, which fixes the $C = +$ assignment, and to determine the $X(3872) \rightarrow \pi^0 \pi^0 J/\psi$ branching fraction.

Experiments should continue to search for additional narrow charmonium states in neutral combinations of charmed mesons and anticharmed mesons. The most likely candidates correspond to the 1^3D_3 , 1^3D_2 , and 1^3F_4 levels [8]. The analysis we have carried out can be extended to the $b\bar{b}$ system, where it may be possible to see discrete threshold-region states as well. For any of these new states that are threshold bound states their mass is primarily determined by the positions of open-flavor channels. For example, if the $X(3872)$ arises through additional interaction in the two-meson sector, then in the $b\bar{b}$ system we would expect an analog state not far below $B^*\bar{B}$ threshold.

ACKNOWLEDGMENTS

We thank our experimental colleagues for stimulating discussions. K.L.'s research was supported by the Department of Energy under Grant No. DE-FG02-91ER40676. Fermilab is operated by Universities Research Association Inc. under Contract No. DE-AC02-76CH03000 with the U.S. Department of Energy.

-
- [1] S. K. Choi *et al.* (BELLE Collaboration), Phys. Rev. Lett. **89**, 102 001 (2002); **89**, 129 901(E) (2002).
 - [2] J. L. Rosner *et al.* (CLEO Collaboration), Phys. Rev. Lett. **95**, 102 003 (2005).
 - [3] P. Rubin (CLEO Collaboration), Phys. Rev. D **72**, 092004 (2005).
 - [4] S. K. Choi *et al.* (BELLE Collaboration), Phys. Rev. Lett. **91**, 262 001 (2003).
 - [5] D. Acosta *et al.* (CDF II Collaboration), Phys. Rev. Lett. **93**, 072 001 (2004).
 - [6] V. M. Abazov *et al.* (D0 Collaboration), Phys. Rev. Lett. **93**, 162 002 (2004).
 - [7] B. Aubert *et al.* (BABAR Collaboration), Phys. Rev. D **71**, 071103 (2005).
 - [8] E. J. Eichten, K. Lane, and C. Quigg, Phys. Rev. D **69**, 094019 (2004).
 - [9] E. J. Eichten, K. Lane, and C. Quigg, Phys. Rev. Lett. **89**, 162 002 (2002).
 - [10] T. Barnes and S. Godfrey, Phys. Rev. D **69**, 054008 (2004).
 - [11] T. Barnes, S. Godfrey, and E. S. Swanson, Phys. Rev. D **72**, 054026 (2005).
 - [12] K. Abe *et al.* (BELLE Collaboration), Phys. Rev. Lett. **94**, 182 002 (2005).
 - [13] K. Abe, *et al.* (BELLE Collaboration), hep-ex/0507019.
 - [14] S. Uehara, *et al.* (BELLE Collaboration), hep-ex/0512035.
 - [15] B. Aubert *et al.* (BABAR Collaboration), Phys. Rev. Lett. **95**, 142 001 (2005).
 - [16] B. Aubert *et al.* (BABAR Collaboration), Phys. Rev. D **73**, 011101 (2006).
 - [17] K. Abe *et al.* (BELLE Collaboration), Phys. Rev. D **70**, 071102 (2004).
 - [18] D. M. Asner *et al.* (CLEO Collaboration), Phys. Rev. Lett. **92**, 142 001 (2004).
 - [19] B. Aubert *et al.* (BABAR Collaboration), Phys. Rev. Lett. **92**, 142 002 (2004).
 - [20] S. Eidelman *et al.*, Phys. Lett. B **592**, 1 (2004) and 2005 partial update for the 2006 edition available at <http://pdg.lbl.gov/>.
 - [21] T. A. Armstrong *et al.*, Phys. Rev. Lett. **69**, 2337 (1992).
 - [22] M. Andreotti *et al.* (Fermilab E835 Collaboration), Phys. Rev. D **72**, 032001 (2005).
 - [23] D. N. Joffe, hep-ex/0505007.
 - [24] K. Gottfried, Phys. Rev. Lett. **40**, 598 (1978).
 - [25] M. B. Voloshin, Nucl. Phys. **B154**, 365 (1979).

- [26] T. M. Yan, Phys. Rev. D **22**, 1652 (1980).
- [27] N. E. Adam (CLEO Collaboration), hep-ex/0508023.
- [28] J. Z. Bai *et al.* (BES Collaboration), Phys. Lett. B **605**, 63 (2005).
- [29] D. H. Miller, hep-ex/0601008.
- [30] K. Abe *et al.* (BELLE Collaboration), Phys. Rev. Lett. **93**, 051 803 (2004).
- [31] B. Aubert *et al.* (BABAR Collaboration), hep-ex/0408083.
- [32] CDF II Collaboration, *The “Lifetime” Distribution of $X(3872)$ Mesons Produced in $\bar{p}p$ Collisions at CDF,* CDF Note 7159.
- [33] CDF Collaboration, *“Measurement of the Dipion Mass Spectrum in $X(3872) \rightarrow \pi^+ \pi^- J/\psi$ Decays,”* CDF Note 05-03-24, <http://www-cdf.fnal.gov/physics/new/bottom/050324.blessed.X/xmPiPi.ps>.
- [34] G. Bauer, hep-ex/0511041.
- [35] M. Suzuki, Phys. Rev. D **72**, 114013 (2005).
- [36] K. Abe *et al.*, hep-ex/0505037.
- [37] J. L. Rosner, Phys. Rev. D **70**, 094023 (2004).
- [38] K. Abe *et al.*, hep-ex/0505038.
- [39] E. Swanson, hep-ph/0509327.
- [40] D. V. Bugg, Phys. Lett. B **598**, 8 (2004); Phys. Rev. D **71**, 016006 (2005). See also Phys. Rep. **397**, 257 (2004).
- [41] N. A. Törnqvist, Phys. Lett. B **590**, 209 (2004).
- [42] F. E. Close and P. R. Page, Phys. Lett. B **578**, 119 (2004).
- [43] E. S. Swanson, J. Phys.: Conf. Ser. **9**, 79 (2005).
- [44] M. B. Voloshin, Phys. Lett. B **579**, 316 (2004).
- [45] L. Maiani, F. Piccinini, A. D. Polosa, and V. Riquer, Phys. Rev. D **71**, 014028 (2005).
- [46] L. Maiani, V. Riquer, F. Piccinini, and A. D. Polosa, Phys. Rev. D **72**, 031502 (2005).
- [47] H. Hogaasen, J. M. Richard, and P. Sorba, hep-ph/0511039.
- [48] F. E. Close and S. Godfrey, Phys. Lett. B **574**, 210 (2003).
- [49] K. J. Juge, J. Kuti, and C. J. Morningstar, Phys. Rev. Lett. **82**, 4400 (1999).
- [50] X. Liao and T. Manke, hep-lat/0210030.
- [51] K. J. Juge, J. Kuti, and C. Morningstar, Phys. Rev. Lett. **90**, 161 601 (2003).
- [52] B. Aubert *et al.* (BABAR Collaboration), Phys. Rev. Lett. **93**, 041 801 (2004).
- [53] R. Giles and S. H. H. Tye, Phys. Rev. D **16**, 1079 (1977).
- [54] W. Buchmuller and S. H. H. Tye, Phys. Rev. Lett. **44**, 850 (1980).
- [55] F. E. Close, Phys. Lett. B **342**, 369 (1995).
- [56] F. E. Close and P. R. Page, Phys. Lett. B **628**, 215 (2005).
- [57] K. Abe *et al.* (BELLE Collaboration), Phys. Rev. Lett. **89**, 142 001 (2002).
- [58] B. Aubert *et al.* (BABAR Collaboration), Phys. Rev. D **72**, 031101 (2005).
- [59] S. L. Zhu, Phys. Lett. B **625**, 212 (2005).
- [60] E. Kou and O. Pène, Phys. Lett. B **631**, 164 (2005).
- [61] E. Braaten and M. Kusunoki, Phys. Rev. D **69**, 074005 (2004).
- [62] M. B. Voloshin and L. B. Okun, JETP Lett. **23**, 333 (1976) [Pis'ma Zh. Eksp. Teor. Fiz. **23**, 369 (1976)].
- [63] A. De Rujula, H. Georgi, and S. L. Glashow, Phys. Rev. Lett. **38**, 317 (1977).
- [64] A. De Rujula and R. L. Jaffe, in *Experimental Meson Spectroscopy 1977*, edited by E. von Goeler and R. Weinstein (Northeastern University Press, Boston, 1977), p. 83.
- [65] E. S. Swanson, Phys. Lett. B **588**, 189 (2004).
- [66] E. Eichten, K. Gottfried, T. Kinoshita, K. D. Lane, and T. M. Yan, Phys. Rev. Lett. **36**, 500 (1976).
- [67] E. Eichten, K. Gottfried, T. Kinoshita, K. D. Lane, and T. M. Yan, Phys. Rev. D **17**, 3090 (1978); **21**, 313(E) (1980).
- [68] E. Eichten, K. Gottfried, T. Kinoshita, K. D. Lane, and T. M. Yan, Phys. Rev. D **21**, 203 (1980).
- [69] N. Brambilla *et al.*, hep-ph/0412158.
- [70] A. Martin and J. M. Richard, Phys. Lett. **115B**, 323 (1982).
- [71] J. L. Rosner, Phys. Rev. D **64**, 094002 (2001).
- [72] J. L. Rosner, Ann. Phys. (N.Y.) **319**, 1 (2005).
- [73] K. K. Seth, hep-ex/0405007.
- [74] E. S. Ackleh, T. Barnes, and E. S. Swanson, Phys. Rev. D **54**, 6811 (1996).
- [75] T. E. Coan *et al.* (CLEO Collaboration), hep-ex/0509030.
- [76] E. Eichten, Phys. Rev. D **22**, 1819 (1980).
- [77] K. Heikkilä, S. Ono, and N. A. Tornqvist, Phys. Rev. D **29**, 110 (1984); **29**, 2136(E) (1984).
- [78] N. Byers and E. Eichten, in *Proceedings of EPS—High Energy Physics '89*, edited by F. Barreiro *et al.* [Nucl. Phys. B (Proc. Suppl.) **16**, 281 (1990)].
- [79] N. Byers, in *Proceedings of Quark Confinement and the Hadron Spectrum*, edited by N. Brambilla and G. M. Prosperi (World Scientific, Singapore, 1995), p. 139.
- [80] Xiaoyan Shen, “Heavy Flavor, Quarkonium Production and Decay,” *Proceedings of Lepton/Photon 2005, Uppsala*, http://lp2005.tsl.uu.se/~lp2005/LP2005/programme/presentationer/3_shen_sxy-lp05.ppt.